

THE INTERNATIONAL SOCIETY OF
PRECISION AGRICULTURE PRESENTS THE
13th INTERNATIONAL CONFERENCE ON
PRECISION AGRICULTURE

July 31-August 4, 2016 • St. Louis, Missouri USA

**Multispectral Imaging and Elevation Mapping from an
Unmanned Aerial System for Precision Agriculture
Applications**

**Christopher Lum, Madison Mackenzie, Charlie Shaw-Feather, Elaiza Luker, and
Matthew Dunbabin**

University of Washington
William E. Boeing Department of Aeronautics
and Astronautics
Guggenheim Hall, Room 211
Box 352400
Seattle, WA 98195-2400

Queensland University of Technology
Institute for Future Environments
Science and Engineering Faculty
2 George Street
Brisbane, Queensland 4000
Australia

**A paper from the Proceedings of the
13th International Conference on Precision Agriculture
July 31 – August 4, 2016
St. Louis, Missouri, USA**

Abstract. As the world population continues to grow, the need for efficient agricultural production becomes more pressing. The majority of farmers still use manual techniques (e.g. visual inspection) to assess the status of their crops, which is tedious and subjective. This paper examines an operational and analytical workflow to incorporate unmanned aerial systems (UAS) into the process of surveying and assessing crop health. The proposed system has the potential to significantly reduce time, labor and cost while also yielding more accurate results, allowing farmers to better estimate their yield and obtain quantifiable data on troubled areas. The airframe for this study was built from a combination of hobby-grade and scientific components. The aircraft incorporate avionics such as a Pixhawk autopilot system, GPS, and data telemetry links. This allows for completely autonomous flight paths to obtain coverage. The main sensor packages evaluated on the UAS for this study were a digital camera and a multi-spectral imager. Overlapping photos were taken during flight to ensure that there were no gaps in data. Post flight the pictures were geo-located in a world fixed frame (e.g. WGS-84). Data was collected across several flight tests conducted in Brisbane, Australia at the Samford Ecological Research Facility (SERF). The primary output was a georeferenced, orthomosaic of the area in the visible light spectrum. Corresponding normalized difference vegetation index (NDVI) maps to assess vegetation health and vigor as well as a digital elevation models (DEM) that represents the terrain's surface in 3D were developed as well. The paper describes the process of obtaining and analyzing these results and compares data products generated using software such as QGIS, MicaSense Atlas, and Agisoft Photoscan Professional. Additionally, analysis accuracy, best practices, and improvements of this type of aerial surveying are discussed.

Keywords. Unmanned aerial system, drone, multispectral imagery, digital elevation data, autonomous survey, flight testing, precision agriculture.

1.0 INTRODUCTION

In catering for a growing, worldwide demand for agricultural goods, the need to improve traditional farming practices with modern methods and technologies has become increasingly evident. Therefore, the facilitation of timely, cost efficient, and accurate operational practices is critical in assessing and managing agricultural production. Precision agriculture (PA) aims to facilitate this process through collecting and evaluating practical, real-time environmental data in order to establish and apply predictive management.

In recent developments of PA, UAS are employed in order to visually inspect crop fields for areas of health and distress. UAS have become prevalent in a variety of military, civil, and commercial applications. The integration of UAS in military operations has seen advantages of greater and safer surveying capacity during mission (Lum, 2009), limiting the risk to human life. In civil applications, the commercialization of UAS technology has improved economic and environmental efficiency and security (Association for Unmanned Vehicle Systems International, 2013).

The United States Federal Aviation Administration (FAA) allows commercial and public entities to operate UAS in the National Airspace System (NAS) on a case-by-case basis via a Certificate of Authorization (COA) or Section 333 exemption (Federal Aviation Administration, 2012). International countries such as Australia plans to follow in suit and legalize the use of commercial UAS (Griffith, 2015). Accompanied by federal support and development, it will soon be common for businesses in the United States and Australia to use UAS to augment human agricultural management activities.

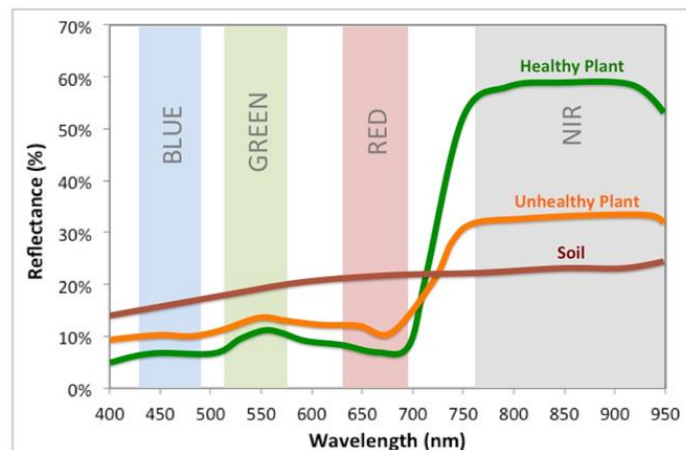


Fig 1. Healthy vegetation has a higher reflectance within the nIR region (MicaSense, 2016).

UAS, coupled with remote sensing techniques like multispectral imaging, are becoming more fundamental within contemporary applications of PA. The use of imaging techniques such as NDVI maps permits higher wavelength data to be detected and used to analyze information more accurately. Plants absorb solar radiation for the process of photosynthesis, and plants absorb more chlorophyll electromagnetic energy within the blue (475nm) and red (660nm) spectrum. A healthy plant often absorbs more energy within the visible spectrum and as a result, the reflectance is lower within the visible range (Fig 1). Fig 1 also shows that healthy vegetation induces a higher reflectance within the near-infrared (nIR) region. This is again due to the presence of chlorophyll within healthy plants as more chlorophyll resists the absorption

of longer wavelengths and hence reflects nIR (Ivanova, Bartsev, Pochekutov, & Kartushinsky, 2006).

These fundamentals enable the use of the NDVI, which uses reflected bands of electromagnetic radiation to determine a scalar measure of plant health and vigor. A standard expression for NDVI is given by Equation 1 (NASA, n.d.).

$$NDVI = \frac{nIR - red}{nIR + red} \quad \text{Equation 1}$$

Where: *NDVI* = *normalized difference vegetation index*

nIR = *near infrared light band*

red = *red light band*

Equation 1 can be used to determine the state of vegetation health and establish plans for management. Remote sensors on UAS can scan crops to look for natural health problems (e.g. need for more water or fertilization), inspect for unexpected diseases, pests, and growth of invasive species (Nixon, 2016). The eventual goal of UAS is to collect data regarding the state of crop and then use it to autonomously control hydration, pesticide, and fertilizer adjusting systems to improve crop health.

UAS research, and the quest to meet this goal, is anticipated to be extremely valuable to the Australian economy as the agriculture industry is valued at roughly \$155 billion, making up 12% of the gross domestic product (GDP) (Australian Bureau of Statistics, 2012). Moreover, UAS research could result in major cost reductions for farmers, thereby permitting reallocation of financial budgets and an increase in GDP relating to agricultural production. The Invasive Animal Cooperative Research Centre and the Australian government have estimated that the cost of feral pests like pigs, wild dogs, and rabbits alone is approximately \$1 billion each year in lost agricultural productivity (Pimentel, Lach, Zuniga, & Morrison, 2002). As a result, UAS devices can provide significant benefits and revolutionize the Australian agriculture industry.

However, widespread use of agricultural UAS is currently restricted by the weight, cost and accessibility of UAS on the market today. Often, the high cost of research and development for crop management is not viable for small-scale agricultural businesses. According to the Australian Bureau of Statistics (ABS), “the majority of Australia’s farms are comparatively small,” with 55% having an estimated value less than \$100,000 in 2010-2011 (Australian Bureau of Statistics, 2012). Therefore, it is necessary to establish a versatile, cost-effective range of UAS that meet Australia’s Civil Aviation Safety Authority’s (CASA) conditions for use within different regions and PA applications.

To investigate feasibility of a low-cost UAS, two aircraft were built by the University of Washington (UW) and the Queensland University of Technology (QUT). These systems were equipped with a basic point-and-shoot digital camera (Canon S100) and a multispectral imager (MicaSense RedEdge) (MicaSense, 2016). The intent is to produce affordable drones that cost \$1000 to \$6500 USD and use 3D mapping and photography to gather data over a specified area. Note that the large variance in price depends on the quality of the sensor carried by the vehicle. The data collected from the UAS can then be used by farmers to alter the surrounding environment and conditions to improve the health of vegetation in the area. By being able to use drones to collect information regarding the health of plants, harvests will correspondingly become more fruitful. While agriculture is expected to make up 80 percent of the potential

market for drones (Wihbey, n.d.), there are additional applications of this research. For example, the UAS developed in this research could also be used for poaching observation, forest fire prevention (Lum, Summers, Carpenter, Rodriguez, & Dunbabin, 2015), and search and rescue (Lum, 2010).

2.0 EXPERIMENTAL HARDWARE AND METHODOLOGY

2.1 Hardware

In this experiment, two autonomous aircraft, named *Exodia* and *Little Wing* (Fig 2), were custom fitted with the previously described imaging sensors and flown over a tree-lined, open field at SERF (Queensland University of Technology, 2015) in Brisbane, Australia, to collect data on the native vegetation using varying imaging techniques. The *Exodia* aircraft was equipped with the MicaSense RedEdge multi-spectral imager while the *Little Wing* aircraft carried a Canon S100 camera. Both UAS were based on a Skywalker 1900 airframe and equipped with a Pixhawk autopilot, a GPS unit, transceivers, and various batteries to run onboard systems. The ground station consisted of a laptop computer running the popular open source Mission Planner software (Osborne, 2016). On *Exodia*, a second GPS was added to provide geotagging information for the MicaSense camera system.

Each imaging sensor was internally mounted in the belly of the aircraft such that it looked downwards in level flight. On *Exodia*, a custom remotely actuated bay door was added to protect the sensor during landing. On *Little Wing*, a Mobius Action Camera was fitted on the forward exterior canopy. This camera transmitted live video to the ground station to monitor the plane's flight from the ground.



Fig 2. *Little Wing* post construction.

2.2 MicaSense Camera (*Exodia* Payload)

The MicaSense RedEdge camera is a five channel multi-spectral imaging system. The five spectrums (image channels) that are captured are: the visible light spectrum of red (660 nm), green (550 nm), and blue (475 nm) as well as two bands of invisible light, namely the red-edge (725 nm), and near-infrared (825 nm). At every image capture, five different images are saved on the SD card in the MicaSense camera. A calibration photo was taken at the start and end of each run to provide corrections for lighting changes during the mission.

2.3 Ground Testing

Ground testing was conducted on QUT's Gardens Point campus where all system sensors and functions were calibrated and tested. Extensive battery tests were also conducted to estimate maximum lifespan during flight. The batteries were estimated provide approximately 30 minutes flight time, placing an upper bound on mission planning. During ground testing, the UAS was also connected to Mission Planner to ensure that the plane could follow waypoints and the software would update in response.

2.4 Experimental Execution

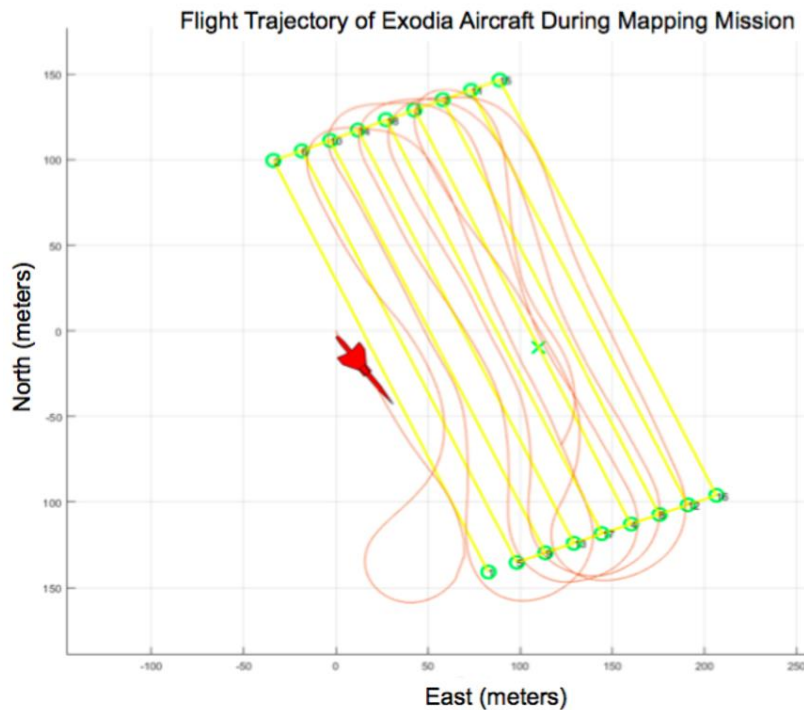


Fig 3. Flight test data showing trajectory of aircraft during a modified parallel track mission.

Each UAS had three experimental trials during which different flight paths were tested. The variations in flight paths were used to gather images from different angles to create a more cohesive collection of aerial survey data. Furthermore, by testing different flight paths, the accuracy and ability of each aircraft to follow pre-planned pathways could be evaluated. The different types of flight paths tested were standard parallel track and creeping line patterns. In addition, a variation of the parallel track pattern where the aircraft skips successive rows and then returns to them later in the flight was tested to allow tighter inter-track spacing while respecting aircraft turn rate constraints (Fig 3).

3.0 DATA REDUCTION

3.1 Flight Logs

Aircraft trajectory was automatically logged using either telemetry logs (tlogs that are communicated to the GCS during a mission) or on board the aircraft using data flash logs. This information was later used in conjunction with Google Maps to create .KML files, which showed the trajectory of the flight paths overlaid on a 3D map of the area. Furthermore, by using information from the logs, the researchers were also able to assess the ability of the aircraft to follow flight paths.

In addition to the tlogs, basic flight logs were recorded. These logs included general information about each of the flights such as, the purpose of each flight, take off times, and descriptions of unforeseen events.

3.2 Image Manipulation

3.2.1 Geotagging

Each photo taken by the Canon S100 was geotagged post flight using position information extracted from the flight log data. The photos acquired by the MicaSense camera were geotagged automatically at the time of acquisition.

Over the three Little Wing flights, the Canon camera captured 115 photos. Using geotagged images, ortho-rectified mosaic images were created. These were primarily processed using Agisoft PhotoScan Professional and visualized using Google Earth.

3.2.2 Preprocessing (Rectification and Cropping)

The MicaSense RedEdge camera takes multi-spectral images by capturing an individual picture at different wavelengths with each of its five lenses. This resulted in over 1,400 in-flight images after three data collection flights. Unnecessary pictures were manually culled from the data set. This resulted in 580 pictures that were suitable for data reduction (corresponding to 116 composite images).

The first step is to rectify each set of five simultaneously captured images. Since each of the lenses are slightly offset and orientated differently from one another, there was a small misalignment between each set of five images for each composite image. The purpose of rectification was to align the images and correct the offset of each lens. This also allowed the multi-spectral data to be consolidated into a single, cohesive, 5-channel image.

Following image rectification, each 5-channel image was cropped to remove non-informative (non-overlapping) portions around its edges (Fig 5).

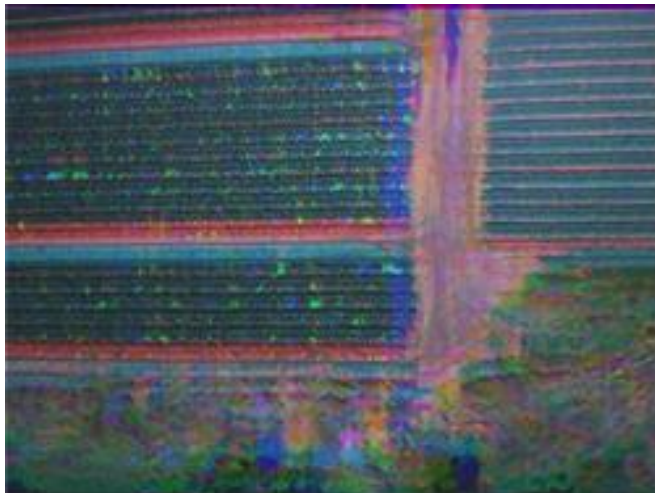


Fig 4. Poor image alignment without rectification. The individual spectral bands do not overlap resulting in a blurred image.

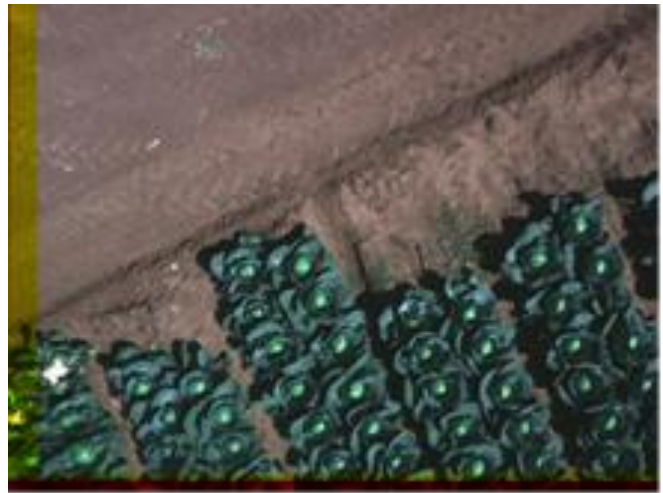


Fig 5. Correct image after image rectification (note that cropping has not yet occurred as seen by the left and lower edges).

The rectified and cropped photos were used to generate NDVI images and ortho-rectified mosaics. The MicaSense Atlas software served as a secondary system to generate maps as well for the purposes of comparison and validation.

3.3 Software

3.3.1 Agisoft Photoscan Professional

Agisoft Photoscan Pro (Agisoft, 2016) was the selected for creating the DEMs and orthomosaics. It has an intuitive workflow that consists of four basic steps: image alignment, dense point cloud formation, mesh creation and texture creation. Minimal user input is required when processing imagery. The main task required by the user is to clip outliers in the dense point cloud stage to minimize the error in the final model.

A software package called CloudCompare (CloudCompare, 2015) allows the user to compare differences in dense point clouds. The quality of medium and high density models created in Photoscan can be analyzed using this freeware.

Both the dense point cloud models created in Agisoft were imported into CloudCompare. The differences between the images were then contrasted with the results shown in Fig. 6. The red represents the medium density model, whereas the yellow represents the high density model. Therefore, with higher rendering quality the model becomes more condensed and has fewer scattered points. As there appeared to be less scattering within the high-density image, it was chosen for analysis.

The blue model on the right, in Fig. 6, shows the medium quality rendered model with the blue section showing the high correlation of points between the high density model. The green shows the points that only have a weak correlation to the high density model. The red points show points in the medium image that have a very weak correlation with the high model (outliers).

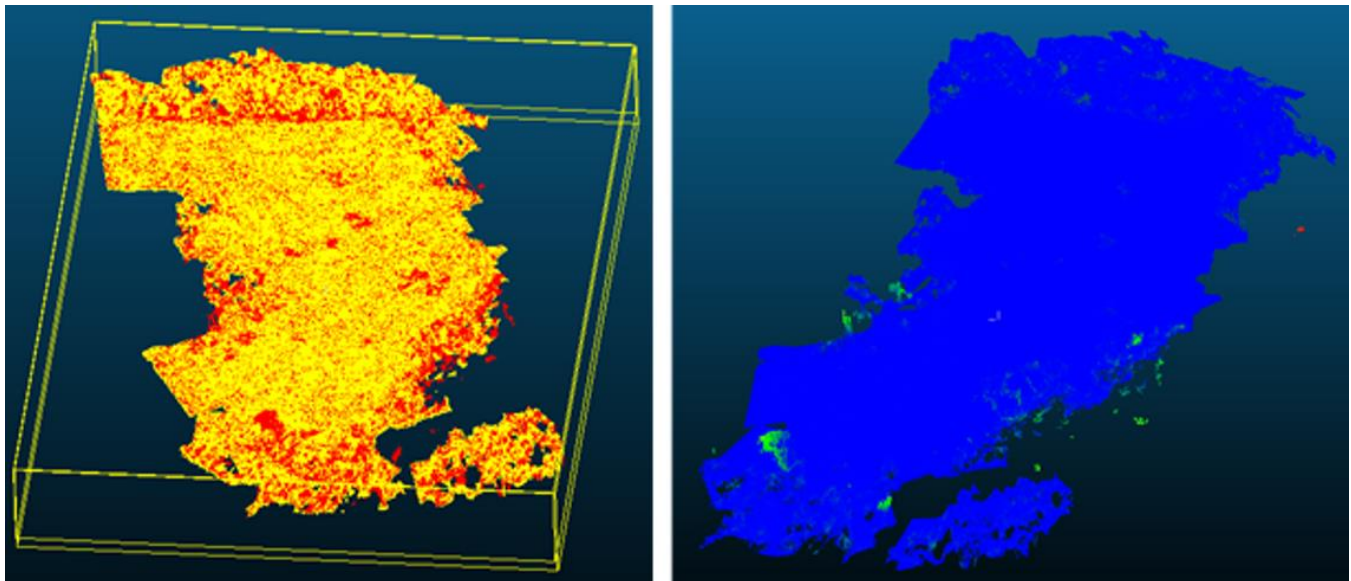


Fig. 6. High & medium density models overlaid (left) and differences in medium density cloud model (right).

3.3.2 Ground Control Points

To have reference points and to increase the GPS accuracy of the model, ground control points (GCPs) were included. Upon adding the GCPs to the model, it became apparent that one of the coordinate systems did not calibrate correctly (see Fig 7). To account for this disparity, the markers in Agisoft were moved to a position that would better reflect the objects. Following this correction, Photoscan then calculated the error in the relevant marker positions. These processes are important in order to rectify anomalies and ensure high GPS accuracy of the model for accurate mapping.



Fig 7. Exposing GPS inaccuracy

Following this correction, Photoscan then calculated the error in the relevant marker positions. Using the calculated errors, the locations of the markers were amended as shown in Fig. 8.

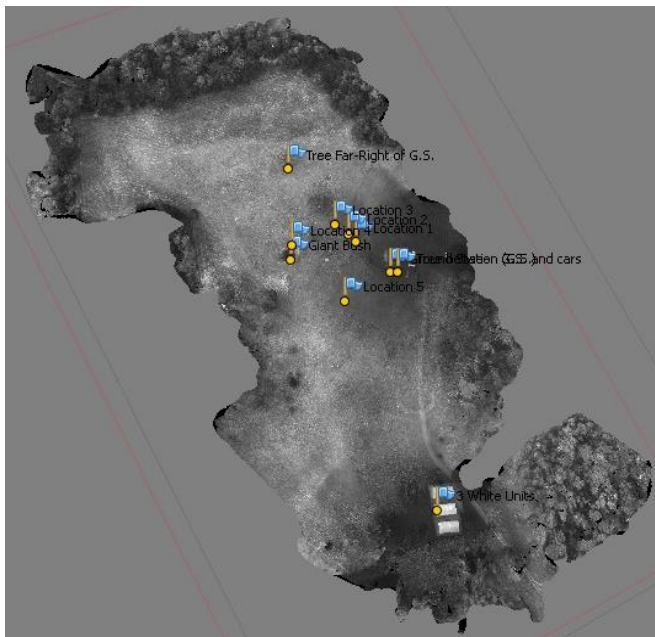


Fig. 8. Ground control points (left) and amended markers (right)

3.3.3 QGIS

Once the data was processed in Agisoft Photoscan Pro, the resulting orthomosaics were then analysed in QGIS (Creative Commons, n.d.). QGIS is a free and open source geographical information system.

The NDVI images were created by selectively showing the light bands using Equation 1; this process yielded a grayscale image. A color map, from green to red, was then applied to the photo. Green represented high NDVI values and healthy vegetation, while red represented low NDVI values and poor vegetation health (Fig 10). The reason why high and low NDVI values represented healthy and unhealthy vegetation, respectively, is that a healthy plant in

the process of photosynthesis will absorb visible light and reflect a significant portion of near-infrared light (SimWright, 2007).

3.3.4 Camera Accuracy and Image Error Estimation

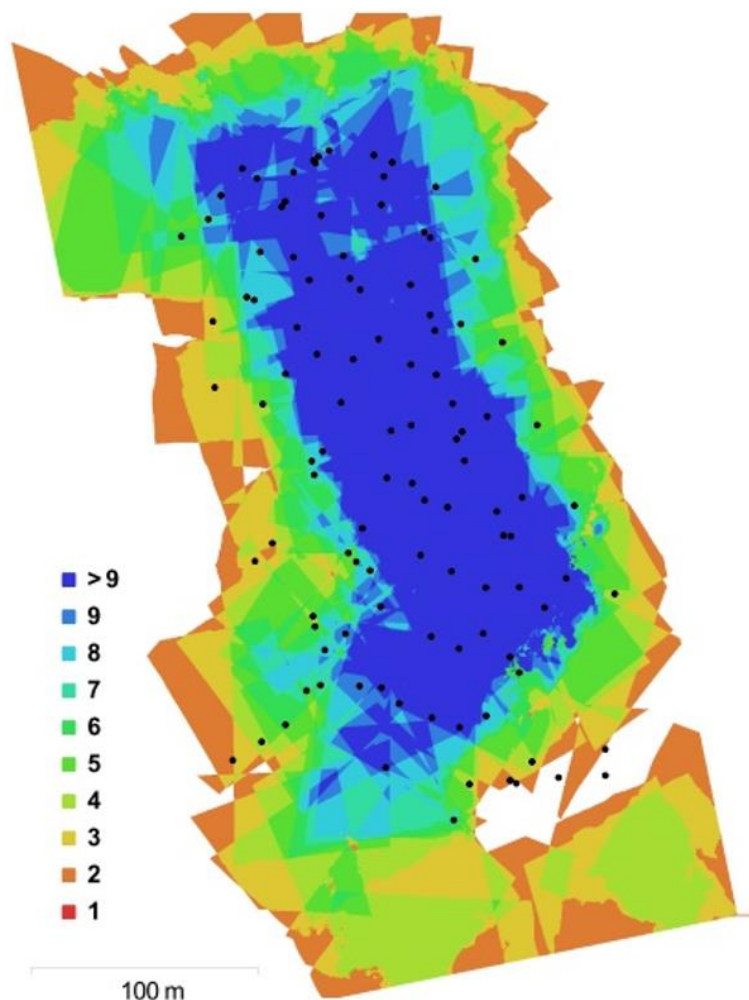


Fig 9. Agisoft generated report on camera overlap.

Photoscan also has the capacity to generate color mapped DEM images, which were used to verify the validity of the results found in QGIS (see Fig 11).

Overlapping images is essential to photogrammetry to gain an accurate orthomosaic. Agisoft recommends +80% forward overlap with a side overlap of 60% (Agisoft, 2016). Shown below in Fig 9 is an image generate by Agisoft that shows the number of overlapping images correlated to their position.

The blue center of the map represents that there were >9 images in that region. In areas where there are less images, hence, less overlap it can be inferred that these regions of the model may be less reliable.

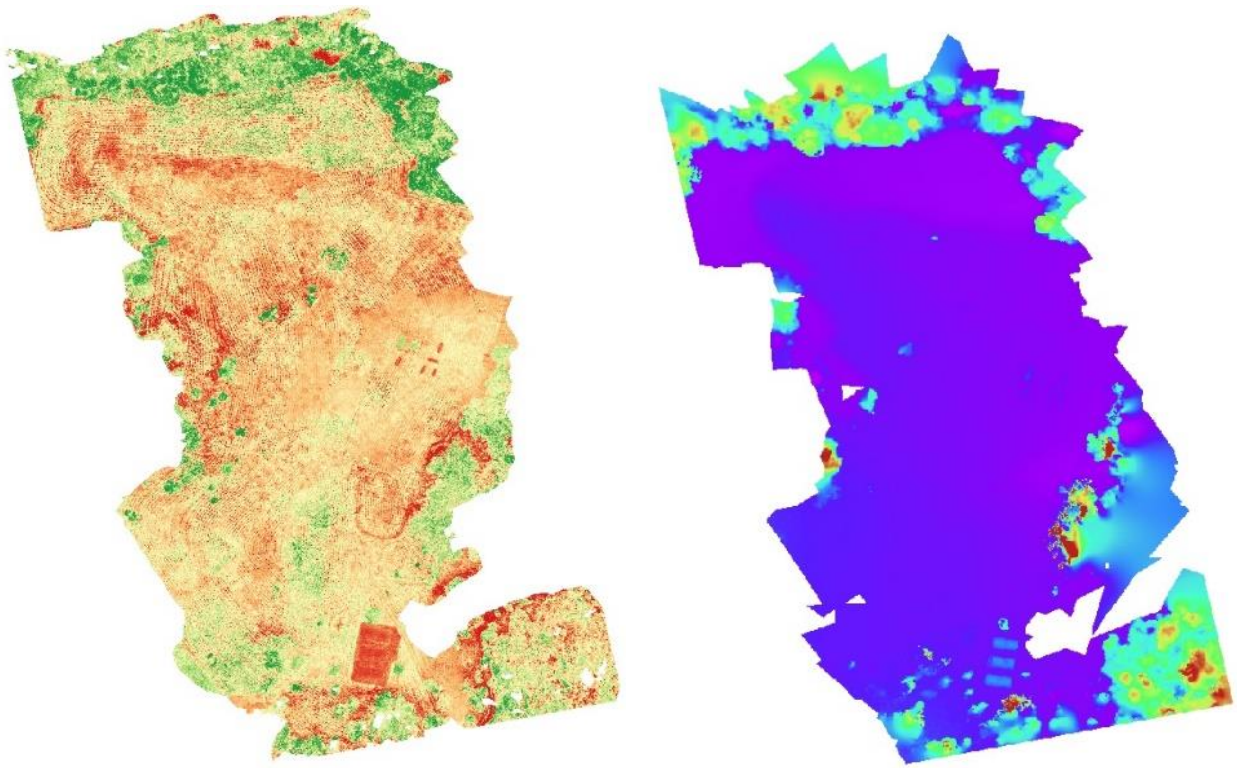


Fig 10. QGIS color mapped NDVI (left) and color mapped DEM (right).

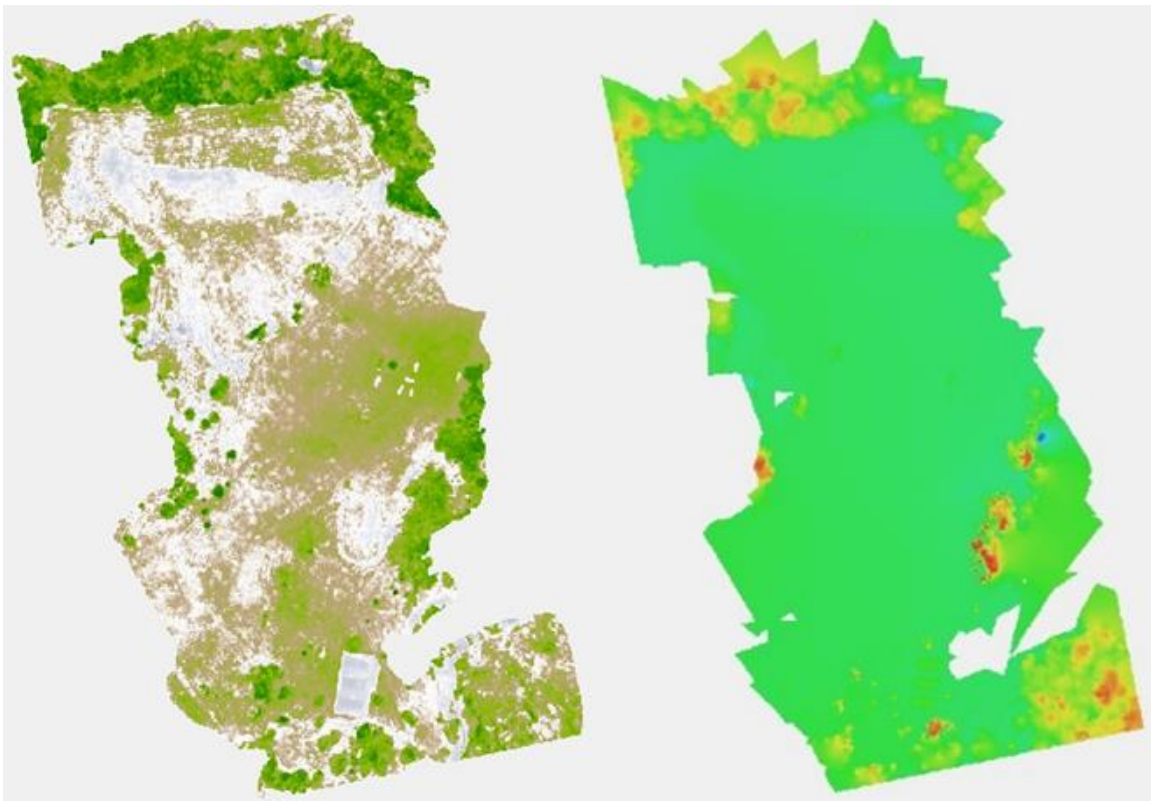


Fig 11. Agisoft Photoscan Pro generated NDVI map (left) and DEM (right).

4.0 RESULTS

The main result of this analysis is a set of NDVI and DEM models of the survey area.

4.1 NDVI Maps

4.1.1 Accuracy

NDVI maps were generated and the data values of the NDVI were extracted from the image to enable crop analysis (Fig 12). In comparison to the professionally created NDVI maps via MicaSense, the images reproduced from Agisoft and QGIS are very similar. The ability to create and manipulate the data without the need of a third party allowed a greater range of flexibility with the output and final data representation.

In order to perform an engineering analysis of multispectral images, Matlab was used to extract the NDVI information from the images reproduced in QGIS.

The analysis from QGIS was compared to the output given by MicaSense to verify the image accuracy and visually compare the NDVI maps. In Fig 14, the two images created are very similar. However, it can be observed that the MicaSense NDVI image detects more subtle variations in vegetation health. Further research could be directed at determining if the QGIS model could be altered to increase its accuracy.

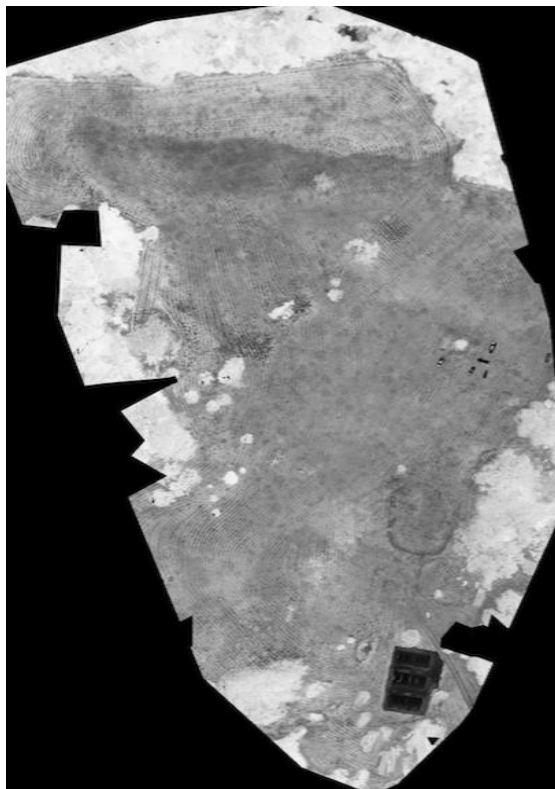


Fig 12. NDVI map generated from the data collected from *Exodia* flight 4

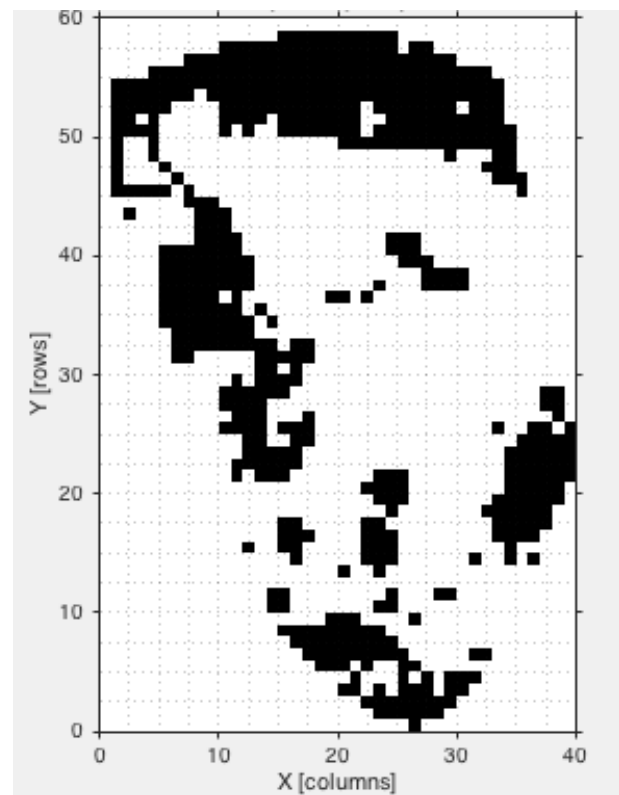


Fig 13. Binary occupancy map corresponding to Fig 12

Post processing allowed NDVI values to be determined at each pixel point, yielding more relevant and practical information. Average NDVI values can be determined over a specified

area for easy recognition of the comparative health of vegetation across different sections of the site. The percentage of vegetation deemed healthy over an area can also be recognized through the specification of appropriate NDVI thresholds.

After obtaining the average NDVI values over a specified area, the quantified data was used in order to generate occupancy maps (Lum, 2006). A binary occupancy map (Elfes, 1989) indicating areas with an average NDVI within the range of 0.6 – 0.8 (in black) was generated (Fig 13).

The NDVI values were also analyzed at each pixel and NDVI values from 0.6 – 0.8 deemed as healthy vegetation were summed to determine a percentage of healthy vegetation (Pettorelli, 2013). Fig 13 indicates that the area surveyed at SERF that has a healthy vegetation percentage of approximately 27.9%. The employment of NDVI to establish percentage of healthy vegetation within an area enables farmers to evaluate and assess the state of their crops, as well as apply methods and strategies to improve yield and quality of agricultural produce.

4.1.2 Validation of Data

The analysis from QGIS was compared to the output given by MicaSense to verify the image accuracy and visually compare the NDVI maps. In Fig 14, the two images created are very similar; however, it can be observed that the MicaSense NDVI image detects more subtle variations in vegetation health.

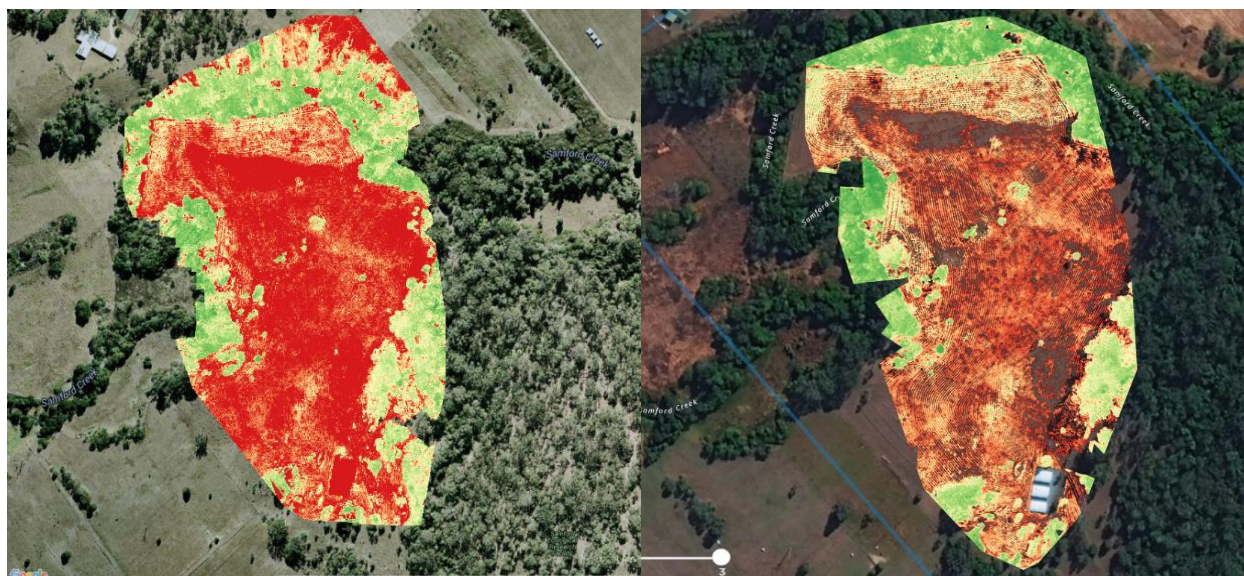


Fig 14. QGIS generated map (left), MicaSense map (right)

4.2 DEM Models

4.2.1 Accuracy

MicaSense generated DEMs were helpful in validate the accuracy of the results. The DEM maps were very similar to those generated by MicaSense and were deemed accurate enough to assist in crop management planning (Fig 15).

4.2.2 Validation of Data

As seen in Fig 16 below, the model created in Agisoft and then further analyzed in QGIS (left) looks very similar to the model provided by MicaSense (right). This means that the UAS and software used (Agisoft, QGIS) to interpret the data from this research was proven successful at determining elevation.

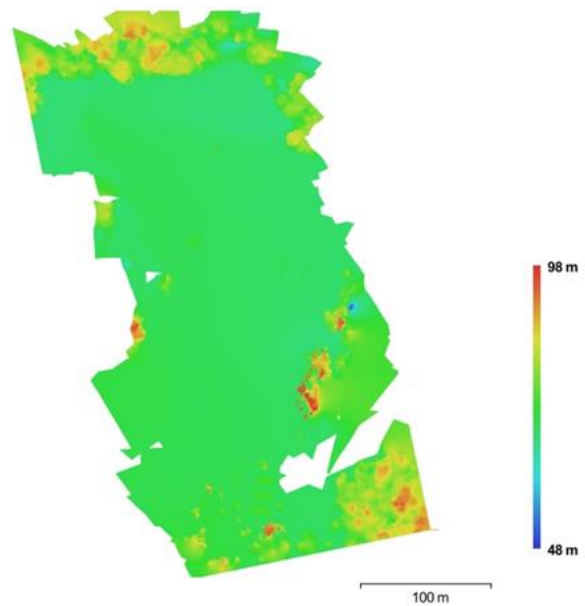


Fig 15. DEM from an Agisoft generated report

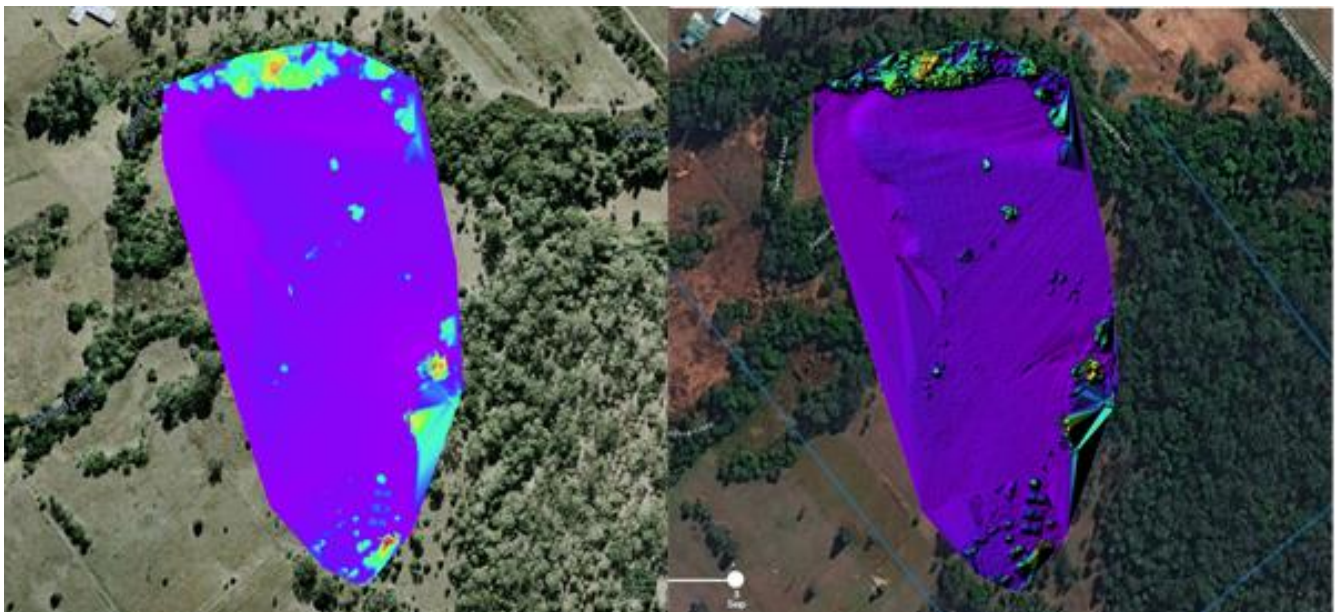


Fig 16. QGIS map (left), MicaSense map (right)

4.3 Estimating Crop Yields

Another useful application of more advanced surveying within the agriculture industry is to estimate crop yield. This was demonstrated within Matlab with the results shown in Fig 17.

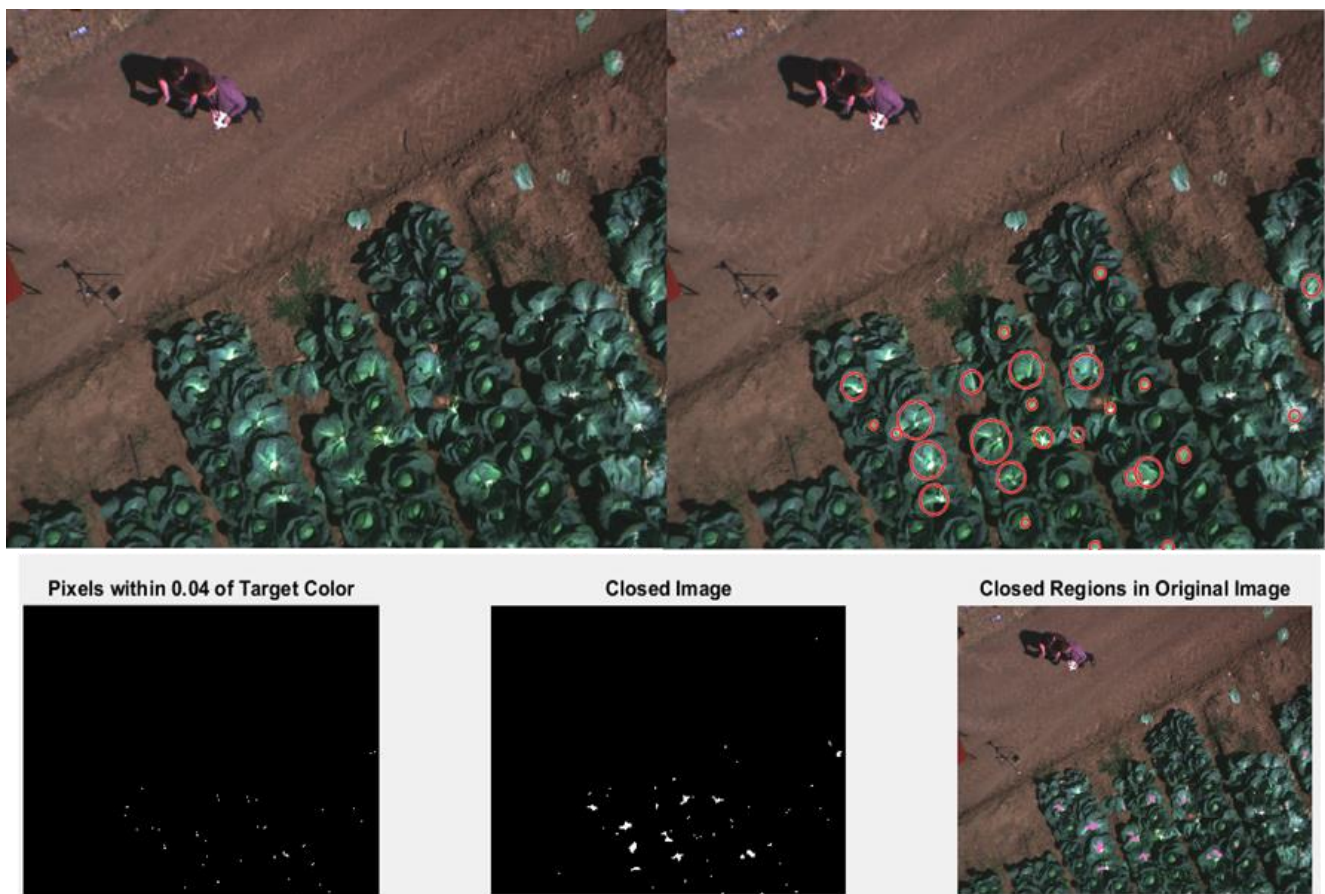


Fig 17. Estimating crop yields. Original image (top left) and image processing algorithm (bottom) used to count total number of crops in image (top right).

This process of systematically counting the number of crop within an image required detecting a distinct pigment (in this case cabbage green). An algorithm would then find clusters of this and circle it to visually depict the crops found by the algorithm (Lum, Summers, Carpenter, Rodriguez, & Dunbabin, 2015).

5.0 DISCUSSION

5.1 Significance of Results and Agricultural Applications

This research has further demonstrated the utility of UAS with an onboard multispectral imager for assessing vegetation health. The applications of such technology, both within and outside agriculture, are extensive. Below are some potential applications and improvements that could be implemented to increase agricultural production (Grassi, 2014):

- Mid-season Crop Health Monitoring: inspect and assess immature crops with NDVI maps.
- Irrigation Equipment Monitoring: examine the nozzles and sprinklers on irrigation equipment to ensure that water is properly being delivered to crops.
- Invasive Species Identification: use NDVI sensor data and image processing to develop a weed map which enables farmers to differentiate between areas of weed infestation and

neighboring healthy crop growth; consequently, they can selectively spray pesticides only on problem areas, minimizing environmental damage and cutting cost.

- Variable-Rate Fertility: use variable-rate application (VRA) maps to determine where the farmer needs to apply more fertilizer to struggling areas and less fertilizer to healthy areas, decreasing fertilizer costs and boosting yields.
- Cattle Herd Monitoring: tracking the quantity and activity level of animals; this is particularly helpful for night-time monitoring as humans cannot see well in the dark.
- Stand uniformity problems: locate and measure areas of irregular or reduced plant stand caused by weather, soil, or planting.
- Moisture monitoring: detect and measure crop stress resulting from too much or too little precipitation or by inadequate draining systems.

The development of UAS technology in parallel with PA has the potential to change the agriculture industry significantly. With the help of UAV technology, farmers will be able to operate at higher profit margins and increase the supply of agricultural resources in the economy, likely encouraging greater affordability of food and supplies.

6.0 CONCLUSION

6.1 Important Report Findings

This paper has described a new hardware and software framework whereby low-cost UAS can be fitted with commercial cameras to generate accurate elevation and NDVI maps of agricultural land. Additionally, a comparison between the results generated by commercial and free-ware software systems has been presented. The orthomosaics created in Agisoft Photoscan Pro were very useful in analyzing the vegetation surveyed at SERF. Agisoft allowed all the separate images taken from the UAS to be stitched together through various photogrammetry techniques.

Furthermore, by using QGIS, vegetation health was able to be assessed in NDVI maps. The results when compared with DEMs obtained from MicaSense were proven to be accurate and reliable.

7.0 ACKNOWLEDGEMENTS

The authors thank Cathryne Jordan, Stephanie Gardner, Jonathan Solomon, Daniel Corona, Nicole Rile, Jessica Trinh, Maximiliano Mantola, Max McDonald, Lara Millman, Able Morales, Hannah Olliges, Jennifer Look, Gizelle Gando, and Anna Pendleton from the University of Washington. This research could also not be completed without the support of the Queensland University of Technology (QUT) and the Australian Research Centre for Aerospace Automation (ARCAA), specifically Gavin Broadbent, Dean Gilligan, Jonathan Kok, and Duncan Campbell.

8.0 References

- 3D point cloud and mesh processing software*. (n.d.). Retrieved from CloudCompare:
<http://www.cloudcompare.org/>
- Agisoft. (2016). *Features Professional Edition*. Retrieved from Agisoft:
<http://www.agisoft.com/features/professional-edition/>

- Agisoft. (2016). *Support Tips & Tricks*. Retrieved from Agisoft:
<http://www.agisoft.com/support/tips-tricks/>
- Association for Unmanned Vehicle Systems International. (2013). *The Economic Impact of Unmanned Aircraft Systems Integration in the United States*.
- Australian Bureau of Statistics. (2012, November 12). *4102.0 - Australian Social Trends, Dec 2012*. Retrieved from Australian Farming and Farmers:
<http://www.abs.gov.au/AUSSTATS/abs@.nsf/Lookup/4102.0Main+Features10Dec+2012>
- Creative Commons. (n.d.). *QGIS - The Leading Open Source Desktop GIS*. Retrieved from QGIS: <http://www.qgis.org/en/site/about/index.html>
- Elfes, A. (1989). *Occupancy Grids: A Probabilistic Framework for Robot Perception and Navigation*. Carnegie Mellon University.
- Federal Aviation Administration. (2013). *FAA's Roadmap for Integration of Civil Unmanned Aircraft Systems (UAS) in the National Airspace System (NAS)*. Washington, DC: Federal Aviation Administration.
- Federal Aviation Administration. (2012). *Section 333 of the FAA Modernization and Reform Act of 2012 (FMRA)*. Washington, DC: Federal Aviation Administration.
- Grassi, M. (2014, December 14). *5 Actual Uses For Drones In Precision Agriculture Today*. Retrieved from DRONELIFE.com: <http://dronelife.com/2014/12/30/5-actual-uses-drones-precision-agriculture-today/>
- Griffith, C. (2015, June 9). *Business boon as CASA set to relax rules for lightweight drones*. Retrieved from The Australian Business Review:
<http://www.theaustralian.com.au/business/technology/business-boon-as-casa-set-to-relax-rules-for-lightweight-drones/news-story/de697f0ea76978f31a26a186f1ebae5b>
- Ivanova, Y. D., Bartsev, S., Pochekutov, A., & Kartushinsky, A. (2006, February 15). The analysis of seasonal activity of photosynthesis and efficiency of various vegetative communities on a basis NDVI for modeling of biosphere processes. *Advances in Space Research*, 39(1), 95-99. Retrieved from Science Direct:
<http://www.sciencedirect.com/science/article/pii/S0273117706000895>
- Lum, C. W., & Vagners, J. (2009). A Modular Algorithm for Exhaustive Map Searching Using Occupancy Based Maps. *Proceedings of the AIAA Infotech@Aerospace Conference*. Seattle: Proceedings of the AIAA Infotech@Aerospace Conference.
- Lum, C. W., Rysdyk, R. T., & Pongpunwattana, A. (2006). Occupancy Based Map Searching Using Heterogeneous Teams of Autonomous Vehicles. *Proceedings of the AIAA Guidance, Navigation, and Control Conference*. Keystone: Proceedings of the AIAA Infotech@Aerospace Conference.
- Lum, C. W., Summers, A., Carpenter, B., Rodriguez, A., & Dunbabin, M. (2015). Automatic Wildfire Detection and Simulation Using Optical Information from Unmanned Aerial Systems. *Proceedings of the 2015 SAE Aerotec Conference*. Seattle.
- Lum, C. W., Vagners, J., & Rysdyk, R. T. (2010). Search Algorithms for Teams of Heterogeneous Agents with Coverage Guarantees. *AIAA Journal of Aerospace Computing, Information, and Communication*, 7(1), 1-31.
- Meier, L. a. (2011). Pixhawk: A system for autonomous flight using onboard computer vision. *Robotics and automation (ICRA), 2011 IEEE international conference on*, (pp. 2992--2997).
- MicaSense. (2016). *RedEdge by MicaSense*. Retrieved from MicaSense:
<http://www.micasense.com/rededge/>

- MicaSense RedEdge NDVI Camera*. (2016). Retrieved from Built Drones:
<http://www.built drones.com/micasense-rededge-ndvi-camera/>
- NASA. (n.d.). *Normalized Difference Vegetation Index (NDVI)*. Retrieved from The Earth Observatory:
http://earthobservatory.nasa.gov/Features/MeasuringVegetation/measuring_vegetation_2.php
- Netting, R. (2014, August 13). *Reflected Near-Infrared Waves*. Retrieved January 4, 2016, from NASA Science: http://missionscience.nasa.gov/ems/08_nearinfraredwaves.html
- Nixon, A. (2016, April 12). *How To Select an Agriculture Drone: An In-Depth Buyer's Guide*. Retrieved from Best Drone for the Job: http://bestdroneforthejob.com/drone-buying-guides/agriculture-drone-buyers-guide/#How_Flying_CamerasMeasure_CropHealth
- Osborne, M. (2016). *Mission Planner Overview*. Retrieved from
<http://ardupilot.org/planner/docs/mission-planner-overview.html>
- Pettorelli, N. (2013). *The Normalized Difference Vegetation Index*. OUP Oxford.
- Pimentel, D., Lach, L., Zuniga, R., & Morrison, D. (2002). Environmental and economic costs associated with non-indigenous species in the United States. *Biological Invasions: Economic and environmental costs of alien plant, animal, and microbe species*, 285-306.
- Queensland University of Technology. (2015, December 14). *SERF Overview*. Retrieved from Queensland University of Technology:
<http://www.serf.qut.edu.au/about/overview/index.jsp>
- SimWright. (2007). *Industries We Support*. Retrieved from SimWright:
<http://simwright.com/industry.htm#cm>
- Weekley, J. G., Wicks, A. L., Reinholtz, C. F., Meehan, K., & Nowak, J. (2007, December 4). *Multispectral Imaging Techniques for Monitoring Vegetative Growth and Health*. Blacksburg, Virginia. Retrieved from <http://scholar.lib.vt.edu/theses/available/etd-11172008-144208/unrestricted/JGWeekleyETD.pdf>
- Wihbey, J. (n.d.). *Agricultural drones may change the way we farm*. Retrieved from The Boston Globe: <https://www.bostonglobe.com/ideas/2015/08/22/agricultural-drones-change-way-farm/WTpOWMV9j4C7kchvbmPr4J/story.html>